



HAL
open science

Flux prediction using artificial neural network (ANN) for the upper part of glycolysis

Anamya Ajjolli Nagaraja, Nicolas Fontaine, Mathieu Delsaut, Philippe Charton, Cedric Damour, Bernard Offmann, Brigitte Grondin-Perez, Frédéric Cadet

► To cite this version:

Anamya Ajjolli Nagaraja, Nicolas Fontaine, Mathieu Delsaut, Philippe Charton, Cedric Damour, et al.. Flux prediction using artificial neural network (ANN) for the upper part of glycolysis. PLoS ONE, 2019, 14 (5), pp.e0216178. 10.1371/journal.pone.0216178 . inserm-02196731

HAL Id: inserm-02196731

<https://inserm.hal.science/inserm-02196731>

Submitted on 29 Jul 2019

HAL is a multi-disciplinary open access archive for the deposit and dissemination of scientific research documents, whether they are published or not. The documents may come from teaching and research institutions in France or abroad, or from public or private research centers.

L'archive ouverte pluridisciplinaire **HAL**, est destinée au dépôt et à la diffusion de documents scientifiques de niveau recherche, publiés ou non, émanant des établissements d'enseignement et de recherche français ou étrangers, des laboratoires publics ou privés.

RESEARCH ARTICLE

Flux prediction using artificial neural network (ANN) for the upper part of glycolysis

Anamya Ajjolli Nagaraja¹, Nicolas Fontaine², Mathieu Delsaut¹, Philippe Charton³, Cedric Damour¹, Bernard Offmann⁴, Brigitte Grondin-Perez¹, Frederic Cadet^{3*}

1 LE2P, Laboratory of Energy, Electronics and Processes EA 4079, Faculty of Sciences and Technology, University of La Reunion, France, **2** PEACCEL, n°6 Square Albin Cachot, Paris, France, **3** DSIMB, INSERM, UMR S-1134, Laboratory of Excellence LABEX GR, Faculty of Sciences and Technology, University of La Reunion & University Paris Diderot, Paris, France, **4** Université de Nantes, Unité Fonctionnalité et Ingénierie des Protéines (UFIP), UMR 6286 CNRS, UFR Sciences et Techniques, chemin de la Houssinière, France

* frederic.cadet.run@gmail.com

Abstract

The selection of optimal enzyme concentration in multienzyme cascade reactions for the highest product yield in practice is very expensive and time-consuming process. The modeling of biological pathways is a difficult process because of the complexity of the system. The mathematical modelling of the system using an analytical approach depends on the many parameters of enzymes which rely on tedious and expensive experiments. The artificial neural network (ANN) method has been successively applied in different fields of science to perform complex functions. In this study, ANN models were trained to predict the flux for the upper part of glycolysis as inferred by NADH consumption, using four enzyme concentrations *i.e.*, phosphoglucosomerase, phosphofructokinase, fructose-bisphosphate-aldolase, triose-phosphate-isomerase. Out of three ANN algorithms, the neuralnet package with two activation functions, “logistic” and “tanh” were implemented. The prediction of the flux was very efficient: RMSE and R^2 were 0.847, 0.93 and 0.804, 0.94 respectively for logistic and tanh functions using a cross validation procedure. This study showed that a systemic approach such as ANN could be used for accurate prediction of the flux through the metabolic pathway. This could help to save a lot of time and costs, particularly from an industrial perspective. The R-code is available at: <https://github.com/DSIMB/ANN-Glycolysis-Flux-Prediction>.

OPEN ACCESS

Citation: Ajjolli Nagaraja A, Fontaine N, Delsaut M, Charton P, Damour C, Offmann B, et al. (2019) Flux prediction using artificial neural network (ANN) for the upper part of glycolysis. PLoS ONE 14(5): e0216178. <https://doi.org/10.1371/journal.pone.0216178>

Editor: Marie-Joelle Virolle, Université Paris-Sud, FRANCE

Received: January 28, 2019

Accepted: April 15, 2019

Published: May 8, 2019

Copyright: © 2019 Ajjolli Nagaraja et al. This is an open access article distributed under the terms of the [Creative Commons Attribution License](https://creativecommons.org/licenses/by/4.0/), which permits unrestricted use, distribution, and reproduction in any medium, provided the original author and source are credited.

Data Availability Statement: All relevant data are within the manuscript and its Supporting Information files.

Funding: AAN is supported by a PhD grant from Region Reunion and European Union (FEDER) under European operational program INTERREG V-2014-2020 file number 20161449, tiers 234273.

Competing interests: The authors have declared that no competing interests exist.

Introduction

The emergence of genomics, transcriptomics and proteomics, along with improvements in information technology, helped us to integrate the information, build the mathematical *in silico* model of a biological system and observe its behaviour [1–5]. The integration of different “-omics” data helped us to understand the genetic difference between the phenotypes, to identify the molecular signature [6,7] and use metabolic engineering [8,9] etc. There have been many attempts to model biological systems, like *Saccharomyces cerevisiae* [4,10–12], *Escherichia coli* [13–15], other organisms [3] and many plant metabolic networks for observing and predicting the behaviour of a system using different methods [2,16].

Abbreviations: ANN, artificial neural network; PGI, phosphoglucosomerase; PFK, 6-phosphofructokinase; FBA, fructose bisphosphate aldolase; TPI, triose phosphate isomerase; RMSE, root mean square error.

Many different kinds of mathematical models exist to study biological systems [17,18]. Several approaches have been developed to determine or estimate the flux through the metabolic pathway [19–21]. Based on the data and constraints used, the mathematical modelling can be classified into two broad categories [2,16] i.e., kinetic modelling or mechanistic modelling [22–24], and constraint-based or stoichiometric modelling [12,25,26]. The kinetic model defines the reaction mechanism in the system using kinetic parameters to evaluate rate laws. These rate laws are defined from the experiment, assuming that the experimental conditions are similar to *in-vivo* conditions [27]. To build a kinetic model, the system has been made as simple as possible, while retaining system behaviour. The modelling of enzymes like phosphofructokinase could be problematic and might need more parameters than other enzymes [28]. Determining the kinetic parameter is expensive and time consuming; some parameters could be more difficult to measure. Although many enzymatic assays are described in the literature, sometimes it is necessary to modify the assay for new enzymes or to find a new one. In some cases, for example, following enzyme reaction through spectrophotometers or spectrofluorimeters, this is difficult due to no absorption or emission signals [29] linked to the reactants. Most of the available kinetic data are obtained from *in-vitro* studies using purified enzymes which might not represent the exact properties of *in-vivo* enzymes [23]. For example: The V_{\max} value measured *in vitro* may not represent the value of an *in vivo* system because of the destruction of enzyme complexes, cellular organisation and the absence of an unknown inhibitor or activator [30,31]. A constraint-based model uses physicochemical constraints like mass balance, thermodynamic constraints, etc., in the modelling, to observe and study the behaviour of the system [25]. There are different methods, like flux balance analysis [32] and metabolic flux analysis [33]. Flux balance analysis is an approach to studying biochemical networks on a genomic scale, which includes all the known metabolite reactions, and the genes that encode for a particular enzyme. The data from genome annotation or existing knowledge is used to construct the network [5,34] and the physicochemical constraints are used to predict the flux distribution, considering that the total product formed must be equal to the total substrate consumed in steady state conditions [32]. This method is used to predict the growth rate [5,32,34,35] or the production of a particular metabolite [36]. Metabolic flux analysis, an experimental based method, allows the quantification of metabolite in the central metabolism using the Carbon-labelled substrate [33,37,38]. The labelled substrate is allowed to distribute over the metabolic network and is measured using NMR [39] or mass spectrometry [32].

Many of the biomolecules like organic acids [40,41], antibiotics [42–44], bioethanol etc. [45,46] have been used in the pharmaceutical and food industries and as energy sources. Biomolecule production is attracting the attention of biologists and industries due to the decrease in non-renewable resources and global warming [47,48]. Synthetic biology and systems biology help to obtain the highest yield of biomolecules from the source [49–51].

Glycolysis is the centre of the metabolic system in all living organisms. It is an anaerobic pathway present in almost all living cells and helps in ATP generation. Glycolysis has been established as the central core for the fermentation. It contributes to the production of different metabolites, like citric acid, succinic acid, amino acids, etc., through pyruvate, the end product of glycolysis [52].

The neural network is an architecture, modelled on the brain, that is organized with neurons and synapses present in a structure of nodes (formal neuron) connected together [53,54]. Each numerical input corresponds to the input layer, and the value to predict (variable to explain) corresponds to the last level, the output layer. Between those two layers, intermediary nodes are present, built specifically and in sufficient number to model the problem; they form the hidden layer. The neural network has been successfully applied in different fields of science such as physics [55,56], environmental science [57–59] and data mining [60,61] for the

prediction of different features in the system. The ANN is also core for deep learning [62]. The artificial neural network could be used to predict the product outcome (i.e. flux through the pathway) when combined with Flux balance analysis or other modelling approaches.

The ANN has been used earlier in predicting the fluxes from ¹³C labelling of metabolites in mammalian gluconeogenesis by M.R. Antoniewicz et al. [21]. Three linear regression modelling methods, multiple linear regression (MLR), principal component regression (PCR) and partial least square regression (PLS) were run on simulated data and compared to the ANN. The study showed that ANN, that requires the larger sample (>200) performed better than the other methods for flux prediction using new mass isotopomer data [21].

Due to the challenges in estimating the flux using different methods like constraint-based and kinetic-based modelling approaches [63–66], we developed a simple method using artificial neural networks. This method is based purely on the existing experimental data and hence does not require kinetic parameters as in kinetic modelling and no prior information is required regarding the stoichiometry of the metabolic pathway. In this study, an artificial neural network was built to estimate the flux using enzyme concentrations for the upper part of glycolysis as input. Finding the optimum enzyme concentration—which gives the highest product—through experiments is very tedious and expensive. The neural network approach could be helpful for choosing the optimum enzyme concentrations which enhance the final product concentration without experimental setup, within a short period of time. Experiments were carried out in order to: *i*) assess the structure of the ANN using three different approaches, *ii*) evaluate different activation functions and *iii*) compare the prediction of flux of NAD⁺ to the fluxes predicted by Fievet & al. (2006).

Materials and methods

Principle of artificial neural networks

The base element of ANN is the perceptron, defined in 1958 by Rosenblatt [67]. A combination function computes a value based on the input layer and some weights. This is a weighted sum $\sum n_i p_i$ (observed node) of the n_i values in the input layer. To define the output value, a function called activation function is applied to this value. We note n_i for the node i , the weight p_i corresponds to the connection between node i , the observed node and the activation function f , associated with the observed node (Fig 1).

The structure of an ANN is defined by the number of layers and nodes, by the way they are linked (activation function) and the method to estimate the weights.

Input for building the ANN model

The flux measurement data from *in-vitro* reconstructed upper part of glycolysis [20] was used to build the artificial neural network (Fig 2). The input for the ANN model consists of concentrations of enzymes phosphoglucosomerase (PGI), phosphofructokinase (PFK), fructose

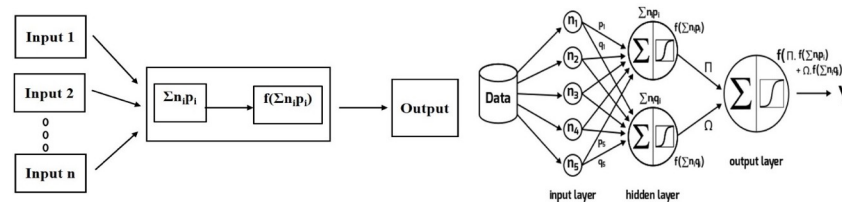


Fig 1. Architecture of artificial neural network.

<https://doi.org/10.1371/journal.pone.0216178.g001>

bisphosphate aldolase (FBA) and triose phosphate isomerase (TPI) in mg/L, and the output is flux J ($\mu\text{M/s}$) measured as the NADH consumption by glycerol-3-phosphate dehydrogenase (G3PDH). The flux measured through the upper part of glycolysis is indirect and we assume that most of the NADH in the system is consumed during the measurement. The data has been normalised using min-max method before building the neural network.

Experimental details

The upper part of glycolysis was reconstructed *in vitro* (Fig 2), with constant concentration of hexokinase and glycerol-3-phosphate dehydrogenase, while the other four enzymes (PGI, PFK, FBA and TPI) concentrations varied. The total enzyme concentration of the four enzymes (PGI, PFK, FBA and TPI) was constant at 101.9 mg/L. The NADH consumption using the glycerol-3-phosphate dehydrogenase is monitored every 2s with Uvikon 850 spectrometer at 390 nm from 60 to 120s. The linear slope of NADH was calculated as the flux through the pathway. The assays were performed in triplicate by Fiévet et al., 2006, at 25 °C, by adding 1mM ATP at pH 7.5. Data is given in supplementary information (Table A in S1 File).

Structure of ANN

The artificial neural network built with a single layer of hidden units [68] using statistical tool R (version 3.4.3) (R Core Team (2013). R: A language and environment for statistical computing. R Foundation for Statistical Computing, Vienna, Austria. <http://www.R-project.org/>) using three different packages: nnet (version 7.3–12) [69], neuralnet (version 1.33) [70] and RSNNS (version 0.4–10) [71].

The network consists of three layers: a) Input (I), b) Hidden layer (H) and c) Output. These layers are connected by edges or neurons. The weighted sum of neuron inputs is submitted to a function which conditions neuron activation. There is no rule for deciding the number of neuron units in a single hidden layer; to choose the best algorithm out of three (i.e. nnet, neuralnet and RSNNS), we first chose the number of hidden units according to Equation 1 and compared the RMSE (Equation 2) and coefficient of determination (R^2) (Equation 3) values between the three methods. The algorithm with the lowest RMSE value and highest R^2 value during the leave-one-out cross validation was chosen as an algorithm of interest and the effect of the number of hidden units on RMSE and R^2 was analysed between 1 to 25 hidden units.

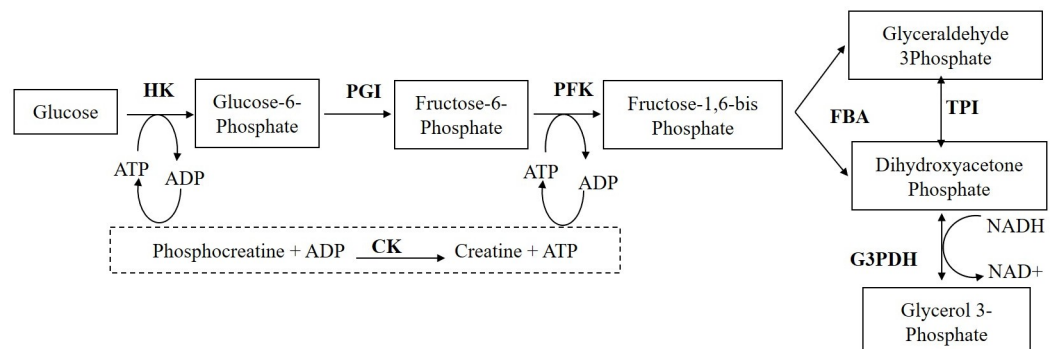


Fig 2. The upper part of glycolysis reconstructed in vitro. HK-hexokinase; PGI-phosphoglucose isomerase; PFK-phosphofructokinase; FBA-fructose bisphosphate aldolase; TPI- triose phosphate isomerase; G3PDH- glycerol-3-phosphate dehydrogenase, CK- Creatine kinase.

<https://doi.org/10.1371/journal.pone.0216178.g002>

Equation 1: Where N_h is number of hidden units; N_s : number of sampling in training data; N_i : number of input neurons; N_o : number of output neurons; α : arbitrary scaling factor 2–10.

$$N_h = \frac{N_s}{\alpha (N_i + N_o)}$$

Equation 2: Where RMSE is root mean square error, Y_i is ANN predicted values; y_i is experimental values; n is number of predictions.

$$RMSE = \sqrt{\frac{\sum_{i=1}^n (Y_i - y_i)^2}{n}}$$

Equation 3: Where R^2 is coefficient of determination; Y_i ANN is predicted values; y_i is experimental values; n is number of predictions, \bar{y} is average of experimental values.

$$R^2 = 1 - \frac{\sum_i (y_i - Y_i)^2}{\sum_i (y_i - \bar{y})^2} \text{ where, } \bar{y} = \frac{\sum_{i=1}^n y_i}{n}$$

Results and discussion

The three-neural network algorithms: nnet [69], neuralnet [70] and RSNNS [71] are built with a hidden number of units ranging from 9 to 12, as shown in Equation 1. The RMSE and coefficient of determination were compared between algorithms during leave-one-out cross validation. Out of three algorithms, the neuralnet performed better than the other two (Table B in [S1 File](#)), allowing the option of choosing two different activation functions *i.e.*, logistic (sigmoidal) and tanh (Equation 4 and Equation 5 respectively).

Equation 4: logistic activation function.

$$\text{Logistic}(x) = \frac{1}{1 + e^{-x}}$$

Equation 5: tanh activation function.

$$\text{tanh}(x) = \frac{2}{1 + e^{-2x}} - 1$$

Using the neuralnet model, with “logistic” and “tanh” activation functions, the effect of the number of hidden units on RMSE and R^2 was studied (Fig 3) with a leave-one-out-cross-validation procedure (Table C in [S1 File](#)). The logistic function with 13 hidden units gives a RMSE of 0.847, R^2 of 0.93 and tanh function RMSE of 0.804, and R^2 of 0.94 with 6 hidden units. The R-script to build the ANN with leave-one-out cross validation is given in R-Scripts A in [S1 File](#).

Experimental flux was compared with the ANN predicted flux by leave-one-outcross-validation procedure, using chosen hidden units with logistic and tanh function (Fig 4). The effects of enzyme concentrations on the predicted flux and experimental flux were compared, and found to follow a similar trend (Fig 5).

During the cross validation of the neural network model, a negative flux value was predicted for one combination of enzymes (Table 1: Index-3). This is because, during a leave-one-out procedure (LOOcv), one combination of the four enzymes is not included in the model training and has to be predicted. The negative value shows the poor ability of the ANN model to predict the outliers, *i.e.* a combination that is not close (in terms of PGI, PFK, FBA and TPI concentrations) to those included in the training data set.

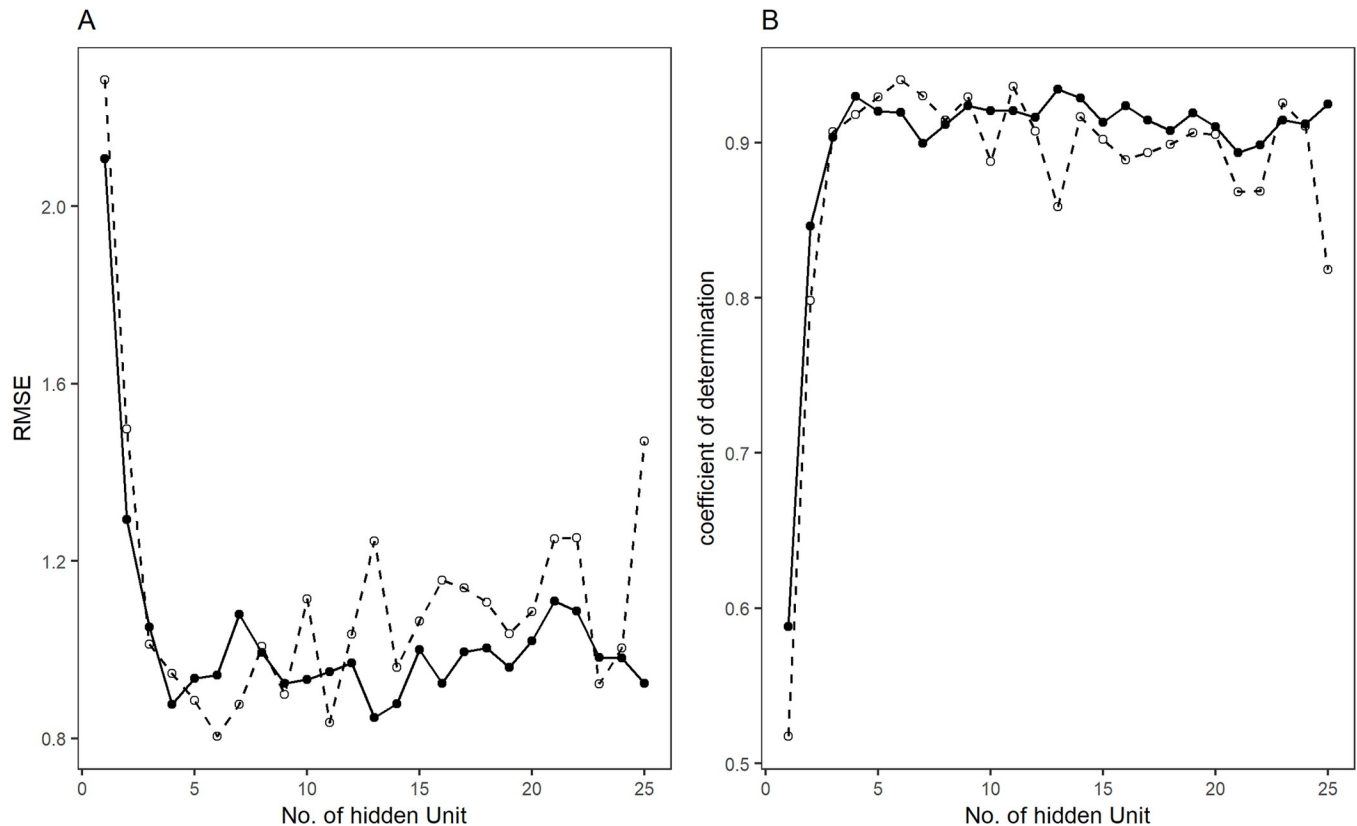


Fig 3. Effect of the number of hidden units on RMSE (A) and coefficient of determination (B) in activation function logistic (filled circle, solid line) and tanh (open circle and dotted lines).

<https://doi.org/10.1371/journal.pone.0216178.g003>

The original study by J. B. Fievet et al. developed a model to predict flux. As the authors mentioned in their article, their flux predictor overestimates the observed flux by a constant factor. The predicted flux in their method, has an R^2 value of 0.86, whereas an ANN approach with logistic function showed an R^2 value to be 0.93 and in case of tanh activation function, an R^2 of 0.94, obtained with leave-one-out cross validation, which implies that the ANN approach is more efficient in predicting the flux than the method developed in the Fievet study. The effect of enzyme concentrations on the predicted flux by both methods follows a similar trend.

The difference between actual flux and ANN predicted flux was an average of 0.57 $\mu\text{M/s}$ for logistic and for tanh, with a standard deviation of 0.63 and 0.57 respectively (Table 1), whereas the Fievet & al. study (2006) showed an average of 3.3 and a standard deviation of 2.2 with actual predicted values. Fievet et al. stated that their method overestimates the flux values by a constant factor of 1.38. Hence by dividing the predicted flux values by 1.38, corrected values were obtained. The new average corrected value is 1.04 and standard deviation is 0.78 with the experimental values. This indicates that the ANN method performs better than the method described in the original study. This ANN-based method provides additional degrees of freedom over the method proposed in Fievet & al. (2006). Indeed, the number of degrees of freedom increases with the number of hidden units. This makes it possible to obtain an important advantage regarding the error inherent to the learning phase.

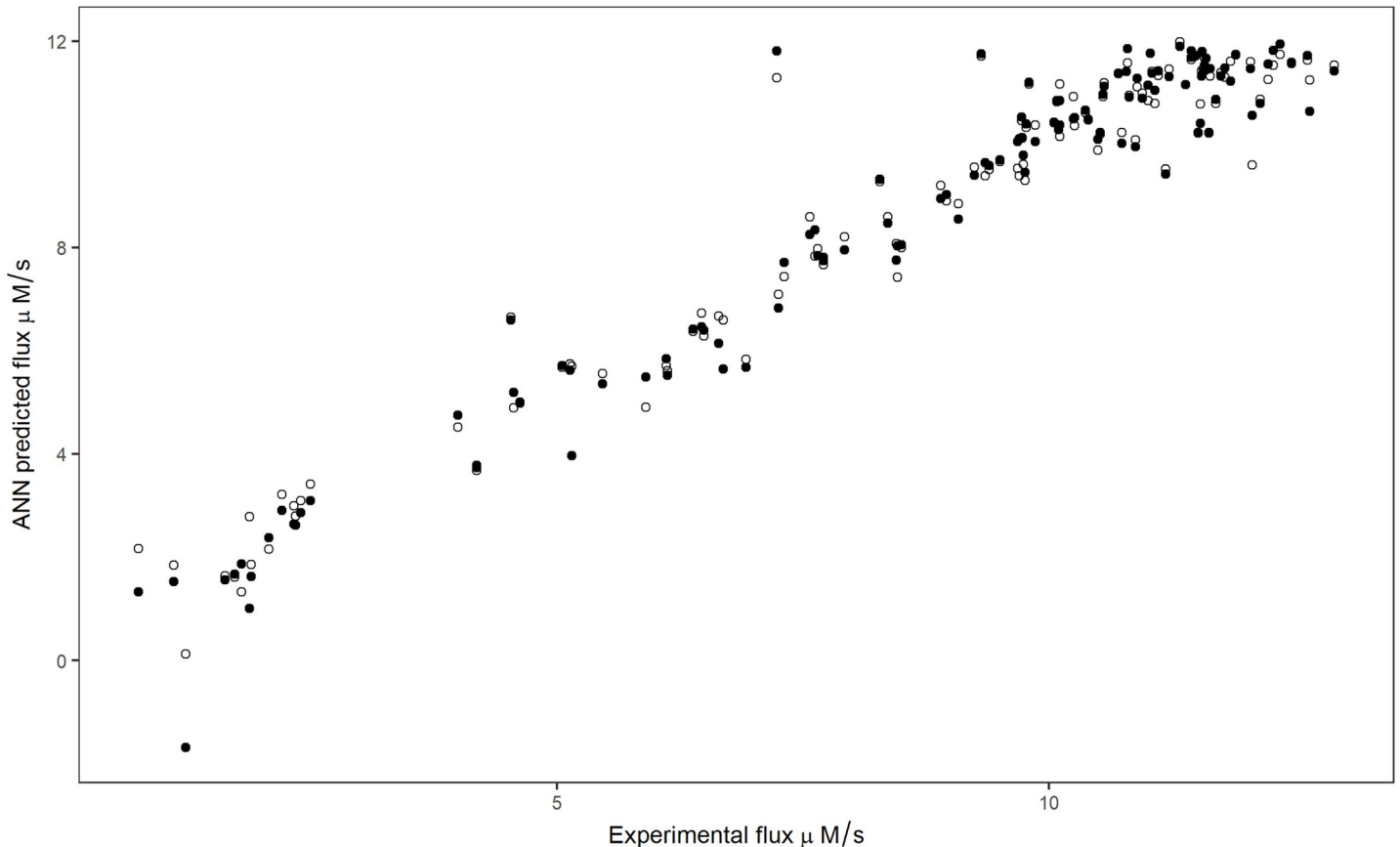


Fig 4. Relationship between flux predicted by leave-one-outcross-validation and experimental flux. Filled and open circles represent logistic and tanh activation functions respectively.

<https://doi.org/10.1371/journal.pone.0216178.g004>

Conclusion

Kinetic modelling of metabolic pathways is challenging because of the difficulties in estimating the kinetic parameters [29,65], and is sometimes expensive because of the high-cost substrates and technologies involved [72,73], whereas the constraint-based model does not use any kinetic parameters but is efficient enough to predict the flux of metabolites. Choosing the optimum enzyme concentrations for the highest flux could be a challenge when conducting experiments. Using artificial intelligence with available experimental data can help us find a quicker and more cost-effective solution for biological problems.

In this study, a neural network model was built successfully with two different activation functions: i.e., logistic (sigmoidal) and tanh, with RMSE and R^2 values of 0.847, 0.93 and 0.804, 0.94 respectively. The difference between actual flux and ANN predicted flux was an average of 0.57 for both activation functions. The J. B. Fievet et al. method after the correction has a RMSE of 1.30, with a 1.05 difference between predicted and observed flux, which clearly indicates that the ANN method works better than the other method.

It has not escaped our attention that the artificial neural network model depends on the diversity of the training data, and hence training the model with a maximum of variability in the concentration of enzymes plays a crucial role. The model built in this study might not be enough to extrapolate a model for all other enzyme concentrations. In future, the study will be

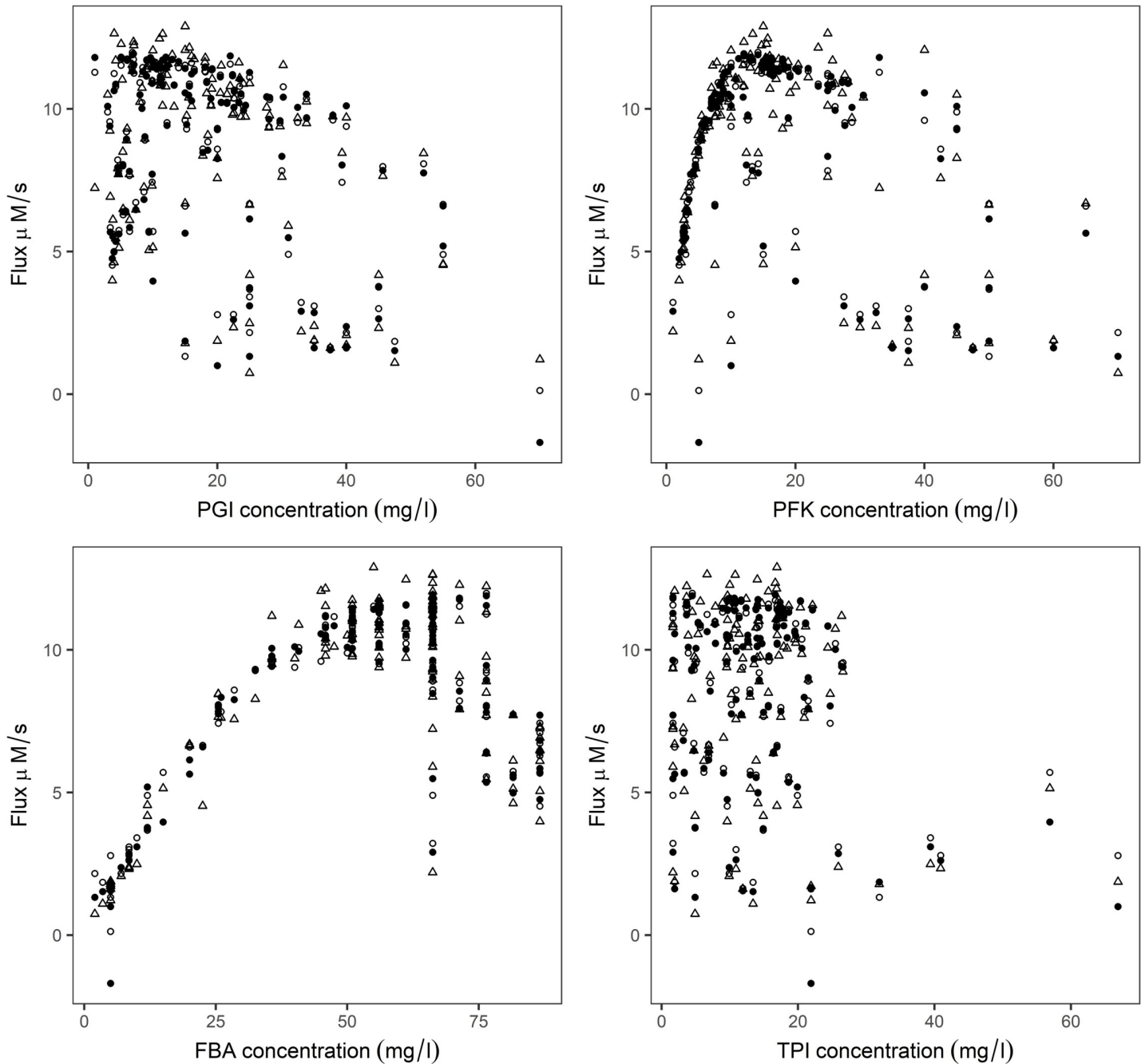


Fig 5. Relationship between the individual enzyme concentration with experimental and ANN predicted flux. Filled circle and open circle are enzyme concentration vs predicted flux with logistic and tanh activation functions respectively, open triangles represent the experiment.

<https://doi.org/10.1371/journal.pone.0216178.g005>

extended to predict the wide range of flux and the enzyme concentration for a particular flux. Experiments in a wet laboratory will be carried out for an upcoming application paper. Even though further work has to be performed, the artificial neural network approach is a promising method in metabolic pathway modelling and could find its place in metabolic engineering and industrial scale biomolecule synthesis.

Table 1. Comparison of flux values (in $\mu\text{M/S}$) between observed flux (J_{Exp}), J.B Fievet (J_{Fievet}) and ANN predicted flux with activation functions logistic ($J_{\text{ANN: logistic}}$) and tanh ($J_{\text{ANN: tanh}}$) and the standard deviation of observed flux (J_{SD}).

Index	J_{Exp}	J_{SD}	J_{Fievet}	$J_{\text{Fievet: Corrected}}$	$J_{\text{ANN: logistic}}$	$J_{\text{ANN: tanh}}$	Difference_ [$J_{\text{Exp}} : J_{\text{Fievet}}$]	Difference_ [$J_{\text{Exp}} : J_{\text{Fievet: Corrected}}$]	Difference_ [$J_{\text{Exp}} : J_{\text{ANN: logistic}}$]	Difference_ [$J_{\text{Exp}} : J_{\text{ANN: tanh}}$]
1	0.74	0.08	1.14	0.83	1.33	2.16	0.4	0.09	0.59	1.42
2	1.1	0.03	1.97	1.43	1.53	1.85	0.87	0.33	0.43	0.75
3	1.22	0.08	2.44	1.77	-1.69	0.13	1.22	0.55	2.91	1.09
4	1.62	0.05	2.79	2.02	1.56	1.64	1.17	0.4	0.06	0.02
5	1.72	0.02	2.78	2.01	1.66	1.62	1.06	0.29	0.06	0.1
6	1.79	0	2.76	2	1.86	1.32	0.97	0.21	0.07	0.47
7	1.87	0.04	2.6	1.88	1	2.79	0.73	0.01	0.87	0.92
8	1.89	0.01	2.8	2.03	1.62	1.85	0.91	0.14	0.27	0.04
9	2.07	0.12	3.86	2.8	2.37	2.16	1.79	0.73	0.3	0.09
10	2.2	0.06	3.08	2.23	2.91	3.22	0.88	0.03	0.71	1.02
11	2.32	0.06	4.63	3.36	2.64	3	2.31	1.04	0.32	0.68
12	2.34	0.1	4.54	3.29	2.62	2.79	2.2	0.95	0.28	0.45
13	2.39	0.21	4.59	3.33	2.86	3.09	2.2	0.94	0.47	0.7
14	2.49	0.07	5.26	3.81	3.1	3.41	2.77	1.32	0.61	0.92
15	3.99	0.13	4.9	3.55	4.76	4.52	0.91	0.44	0.77	0.53
16	4.18	0.22	6.4	4.64	3.73	3.68	2.22	0.46	0.45	0.5
17	4.18	0.15	6.43	4.66	3.78	3.75	2.25	0.48	0.4	0.43
18	4.53	0.65	8.4	6.09	6.6	6.65	3.87	1.56	2.07	2.12
19	4.56	0.06	5.98	4.33	5.2	4.9	1.42	0.23	0.64	0.34
20	4.62	0.06	5.52	4	5	4.99	0.9	0.62	0.38	0.37
21	5.05	0.13	6.77	4.91	5.71	5.68	1.72	0.14	0.66	0.63
22	5.13	0.19	6.27	4.54	5.62	5.74	1.14	0.59	0.49	0.61
23	5.15	0.26	6.98	5.06	3.97	5.7	1.83	0.09	1.18	0.55
24	5.46	0.1	6.09	4.41	5.36	5.55	0.63	1.05	0.1	0.09
25	5.9	0.03	7.75	5.62	5.49	4.9	1.85	0.28	0.41	1
26	6.11	0.15	6.72	4.87	5.84	5.71	0.61	1.24	0.27	0.4
27	6.12	0.12	6.17	4.47	5.53	5.61	0.05	1.65	0.59	0.51
28	6.38	0.29	7.51	5.44	6.42	6.38	1.13	0.94	0.04	0
29	6.47	0.08	7.77	5.63	6.47	6.72	1.3	0.84	0	0.25
30	6.49	0.09	7.09	5.14	6.4	6.29	0.6	1.35	0.09	0.2
31	6.64	0.1	10.19	7.38	6.14	6.67	3.55	0.74	0.5	0.03
32	6.69	0.11	9.95	7.21	5.64	6.59	3.26	0.52	1.05	0.1
33	6.92	0.24	6.2	4.49	5.68	5.84	0.72	2.43	1.24	1.08
34	7.23	0.01	6.3	4.57	11.8	11.29	0.93	2.66	4.57	4.06
35	7.25	0.11	8.36	6.06	6.83	7.09	1.11	1.19	0.42	0.16
36	7.31	0.04	8.92	6.46	7.72	7.44	1.61	0.85	0.41	0.13
37	7.57	0.65	13.45	9.75	8.26	8.59	5.88	2.18	0.69	1.02
38	7.62	0.15	12.05	8.73	8.34	7.83	4.43	1.11	0.72	0.21
39	7.65	0.32	10.72	7.77	7.84	7.98	3.07	0.12	0.19	0.33
40	7.71	0.34	8.27	5.99	7.74	7.74	0.56	1.72	0.03	0.03
41	7.71	0.11	8.86	6.42	7.81	7.67	1.15	1.29	0.1	0.04
42	7.92	0.11	8.59	6.22	7.95	8.21	0.67	1.7	0.03	0.29
43	8.28	0.33	15.02	10.88	9.32	9.28	6.74	2.6	1.04	1
44	8.36	0.15	10.79	7.82	8.48	8.6	2.43	0.54	0.12	0.24
45	8.45	0.23	10.92	7.91	7.76	8.08	2.47	0.54	0.69	0.37

(Continued)

Table 1. (Continued)

Index	J _{Exp}	J _{SD}	J _{Fievet}	J _{Fievet: Corrected}	J _{ANN: logistic}	J _{ANN: tanh}	Difference_ _[J_{Exp} : J_{Fievet}]	Difference_ _[J_{Exp} : J_{Fievet: Corrected}]	Difference_ _[J_{Exp} : J_{ANN:logistic}]	Difference_ _[J_{Exp} : J_{ANN:tanh}]
46	8.46	0.11	10.49	7.6	8.03	7.43	2.03	0.86	0.43	1.03
47	8.5	0.09	8.97	6.5	8.05	8	0.47	2	0.45	0.5
48	8.9	0.06	10.03	7.27	8.94	9.2	1.13	1.63	0.04	0.3
49	8.96	0.08	10.55	7.64	9.03	8.91	1.59	1.32	0.07	0.05
50	9.08	0.35	10.97	7.95	8.56	8.85	1.89	1.13	0.52	0.23
51	9.24	0.04	8.74	6.33	9.4	9.55	0.5	2.91	0.16	0.31
52	9.31	0.1	15.81	11.46	11.75	11.71	6.5	2.15	2.44	2.4
53	9.35	0.46	12.43	9.01	9.64	9.39	3.08	0.34	0.29	0.04
54	9.39	0.22	12.52	9.07	9.59	9.51	3.13	0.32	0.2	0.12
55	9.5	0.18	14.66	10.62	9.7	9.67	5.16	1.12	0.2	0.17
56	9.68	0.14	15.84	11.48	10.05	9.53	6.16	1.8	0.37	0.15
57	9.7	0.55	13.13	9.51	10.11	9.39	3.43	0.19	0.41	0.31
58	9.72	0.18	13.77	9.98	10.53	10.46	4.05	0.26	0.81	0.74
59	9.73	0.11	13.23	9.59	10.13	10.11	3.5	0.14	0.4	0.38
60	9.74	0.05	13.24	9.59	9.79	9.61	3.5	0.15	0.05	0.13
61	9.76	0.03	11.75	8.51	9.45	9.3	1.99	1.25	0.31	0.46
62	9.77	0.13	13.58	9.84	10.4	10.33	3.81	0.07	0.63	0.56
63	9.8	0.27	16.29	11.8	11.2	11.16	6.49	2	1.4	1.36
64	9.86	0.05	12.94	9.38	10.05	10.38	3.08	0.48	0.19	0.52
65	10.05	0.09	13.89	10.07	10.42	10.43	3.84	0.02	0.37	0.38
66	10.08	0.05	13.11	9.5	10.84	10.83	3.03	0.58	0.76	0.75
67	10.1	0.29	13.13	9.51	10.29	10.29	3.03	0.59	0.19	0.19
68	10.11	0.27	13.34	9.67	10.37	10.15	3.23	0.44	0.26	0.04
69	10.11	0.34	16.89	12.24	10.85	11.17	6.78	2.13	0.74	1.06
70	10.25	0.07	12.73	9.22	10.5	10.92	2.48	1.03	0.25	0.67
71	10.26	0.03	13.82	10.01	10.52	10.36	3.56	0.25	0.26	0.1
72	10.37	0.08	13.68	9.91	10.66	10.62	3.31	0.46	0.29	0.25
73	10.4	0.22	17.96	13.01	10.48	10.47	7.56	2.61	0.08	0.07
74	10.5	0.35	12.1	8.77	10.1	9.89	1.6	1.73	0.4	0.61
75	10.52	0.07	13.05	9.46	10.23	10.2	2.53	1.06	0.29	0.32
76	10.55	0.29	19.26	13.96	10.97	10.93	8.71	3.41	0.42	0.38
77	10.56	0.42	17.95	13.01	11.12	11.19	7.39	2.45	0.56	0.63
78	10.71	0.19	17.85	12.93	11.37	11.37	7.14	2.22	0.66	0.66
79	10.74	0.23	11.69	8.47	10.02	10.23	0.95	2.27	0.72	0.51
80	10.79	0.24	17.82	12.91	11.41	11.41	7.03	2.12	0.62	0.62
81	10.8	n,d	17.51	12.69	11.86	11.57	6.71	1.89	1.06	0.77
82	10.82	0.19	13.48	9.77	10.91	11.76	2.66	1.05	0.09	0.94
83	10.88	0.3	16.88	12.23	9.96	10.08	6	1.35	0.92	0.8
84	10.9	0.14	15.48	11.22	11.28	11.11	4.58	0.32	0.38	0.21
85	10.95	0.26	18.48	13.39	10.9	11	7.53	2.44	0.05	0.05
86	11.01	0.16	17.59	12.75	11.14	10.84	6.58	1.74	0.13	0.17
87	11.03	0.16	13.48	9.77	11.77	10.22	2.45	1.26	0.74	0.81
88	11.05	0.29	18.2	13.19	11.38	11.41	7.15	2.14	0.33	0.36
89	11.08	0.25	14.92	10.81	11.05	10.79	3.84	0.27	0.03	0.29
90	11.11	0.07	17.06	12.36	11.42	11.33	5.95	1.25	0.31	0.22

(Continued)

Table 1. (Continued)

Index	J _{Exp}	J _{SD}	J _{Fievet}	J _{Fievet: Corrected}	J _{ANN: logistic}	J _{ANN: tanh}	Difference_ _[J_{Exp} : J_{Fievet}]	Difference_ _[J_{Exp} : J_{Fievet: Corrected}]	Difference_ _[J_{Exp} : J_{ANN:logistic}]	Difference_ _[J_{Exp} : J_{ANN:tanh}]
91	11.19	0.22	14.36	10.41	9.42	9.52	3.17	0.78	1.77	1.67
92	11.22	0.1	13.93	10.09	11.31	11.46	2.71	1.13	0.09	0.24
93	11.33	0.38	16.17	11.72	11.9	11.98	4.84	0.39	0.57	0.65
94	11.39	0.24	13.61	9.86	11.16	11.15	2.22	1.53	0.23	0.24
95	11.45	0.49	16.86	12.22	11.81	11.69	5.41	0.77	0.36	0.24
96	11.45	0.21	17.14	12.42	11.68	11.65	5.69	0.97	0.23	0.2
97	11.49	0.1	15.97	11.57	11.73	11.71	4.48	0.08	0.24	0.22
98	11.52	0.08	13.61	9.86	10.23	10.22	2.09	1.66	1.29	1.3
99	11.54	0.07	14.93	10.82	10.41	10.78	3.39	0.72	1.13	0.76
100	11.55	0.16	15.71	11.38	11.32	11.42	4.16	0.17	0.23	0.13
101	11.56	0.23	17.45	12.64	11.79	11.8	5.89	1.08	0.23	0.24
102	11.57	0.29	16.13	11.69	11.4	11.46	4.56	0.12	0.17	0.11
103	11.58	0.06	16.85	12.21	11.53	11.67	5.27	0.63	0.05	0.09
104	11.6	0	19.32	14	11.66	11.44	7.72	2.4	0.06	0.16
105	11.63	0.14	13.48	9.77	10.23	10.94	1.85	1.86	1.4	0.69
106	11.64	0.05	18.64	13.51	11.46	11.33	7	1.87	0.18	0.31
107	11.7	0.3	14.94	10.83	10.87	10.79	3.24	0.87	0.83	0.91
108	11.75	0.1	17.04	12.35	11.32	11.39	5.29	0.6	0.43	0.36
109	11.79	0.08	17.5	12.68	11.48	11.3	5.71	0.89	0.31	0.49
110	11.85	0.21	18.97	13.75	11.23	11.61	7.12	1.9	0.62	0.24
111	11.9	0.14	17.09	12.38	11.74	11.73	5.19	0.48	0.16	0.17
112	12.05	0.07	14.68	10.64	11.47	11.61	2.63	1.41	0.58	0.44
113	12.07	0.81	18.22	13.2	10.57	9.6	6.15	1.13	1.5	2.47
114	12.15	0.22	17.11	12.4	10.8	10.87	4.96	0.25	1.35	1.28
115	12.23	0.13	16.53	11.98	11.56	11.25	4.3	0.25	0.67	0.98
116	12.28	0.13	14.77	10.7	11.82	11.53	2.49	1.58	0.46	0.75
117	12.35	0.21	14.61	10.59	11.94	11.74	2.26	1.76	0.41	0.61
118	12.47	0.17	17.1	12.39	11.57	11.58	4.63	0.08	0.9	0.89
119	12.63	0.15	16.91	12.25	11.72	11.63	4.28	0.38	0.91	1
120	12.65	0.21	14.5	10.51	10.64	11.24	1.85	2.14	2.01	1.41
121	12.9	0.53	16.79	12.17	11.42	11.53	3.89	0.73	1.48	1.37
Average difference between observed and predicted							3.32	1.05	0.57	0.57
Standard deviation of the difference between observed and predicted							2.14	0.78	0.63	0.57

<https://doi.org/10.1371/journal.pone.0216178.t001>

Supporting information

S1 File. Table A: Input used to build artificial neural network from Fievet et al., 2016. Table B: Comparison of RMSE and R-squared values during the leave-one-out crossvalidation between neuralnet, nnet and RSNNS algorithm. Table C: RMSE and R-squared for values between the activation functions logistics and tanh during leave-one-out cross validation for the neuralnet method. R-Scripts A: R-script used to obtained the [Table 1](#). The different activation function and number of hidden units are selected using "act.fct = " and "hidden = ". (DOCX)

Acknowledgments

AAN is supported by a PhD grant from the Region Reunion and European Union (FEDER) under European operational program INTERRG V-2014-2020 file number 20161449, tiers 234273.

Author Contributions

Investigation: Anamya Ajjolli Nagaraja, Nicolas Fontaine, Mathieu Delsaut, Philippe Charton, Cedric Damour, Bernard Offmann, Brigitte Grondin-Perez.

Methodology: Philippe Charton, Cedric Damour, Frederic Cadet.

Supervision: Philippe Charton, Cedric Damour, Frederic Cadet.

Writing – original draft: Anamya Ajjolli Nagaraja, Nicolas Fontaine, Mathieu Delsaut, Philippe Charton, Cedric Damour, Bernard Offmann, Brigitte Grondin-Perez, Frederic Cadet.

Writing – review & editing: Anamya Ajjolli Nagaraja, Nicolas Fontaine, Mathieu Delsaut, Philippe Charton, Cedric Damour, Bernard Offmann, Brigitte Grondin-Perez, Frederic Cadet.

References

1. Fukushima A, Kusano M, Redestig H, Arita M, Saito K. Integrated omics approaches in plant systems biology. *Curr Opin Chem Biol.* 2009; 13(5–6):532–8. <https://doi.org/10.1016/j.cbpa.2009.09.022> PMID: 19837627
2. Stelling J. Mathematical models in microbial systems biology. *Curr Opin Microbiol.* 2004; 7(5):513–8. <https://doi.org/10.1016/j.mib.2004.08.004> PMID: 15451507
3. Pereira B, Miguel J, Vilaça P, Soares S, Rocha I, Carneiro S. Reconstruction of a genome-scale metabolic model for *Actinobacillus succinogenes* 130Z. *BMC Syst Biol.* 2018; 12.
4. Nookaew I, Olivares-Hernández R, Bhumiratana S, Nielsen J. Genome-Scale Metabolic Models of *Saccharomyces cerevisiae*. In: *Methods in molecular biology* (Clifton, NJ) [Internet]. 2011. p. 445–63. Available from: <http://www.ncbi.nlm.nih.gov/pubmed/21863502>
5. Schilling CH, Covert MW, Famili I, Church GM, Edwards JS, Palsson BO. Genome-Scale Metabolic Model of *Helicobacter pylori* 26695. *J Biotechnol.* 2002; 184(16):4582–93.
6. Acharjee A, Kloosterman B, Visser RGF, Maliepaard C. Integration of multi-omics data for prediction of phenotypic traits using random forest. *BMC Bioinformatics* [Internet]. 2016; 17(5):363–73. Available from: <http://dx.doi.org/10.1186/s12859-016-1043-4>
7. Craig E, Wheelock VG, David Balgoma BN, Brandsma J, Paul J, Skipp, Stuart Snowden Dominic Burg, D'Amico A, Ildiko Horvath, et al. Application of 'omics technologies to biomarker discovery in inflammatory lung diseases. *Eur Respir J.* 2013; 42(3):802–25. <https://doi.org/10.1183/09031936.00078812> PMID: 23397306
8. Vemuri GN, Aristidou AA. Metabolic Engineering in the -omics Era: Elucidating and Modulating Regulatory Networks. *Microbiol Mol Biol Rev.* 2005; 69(2):197–216. <https://doi.org/10.1128/MMBR.69.2.197-216.2005> PMID: 15944454
9. Chen GQ. Omics Meets Metabolic Pathway Engineering. *Cell Syst* [Internet]. 2016; 2(6):362–3. Available from: <https://doi.org/10.1016/j.cels.2016.05.005> PMID: 27237740
10. Duarte NC, Herrgård MJ, Palsson BØ. Reconstruction and validation of *Saccharomyces cerevisiae* iND750, a fully compartmentalized genome-scale metabolic model. *Genome Res* [Internet]. 2004 Jul; 14(7):1298–309. Available from: <https://doi.org/10.1101/gr.2250904> PMID: 15197165
11. Förster J, Famili I, Fu P, Palsson BØ, Nielsen J. Genome-scale reconstruction of the *Saccharomyces cerevisiae* metabolic network. *Genome Res* [Internet]. 2003 Feb; 13(2):244–53. Available from: <http://www.ncbi.nlm.nih.gov/pubmed/12566402> <https://doi.org/10.1101/gr.234503> PMID: 12566402
12. Price ND, Reed JL, Palsson B. Genome-scale models of microbial cells: Evaluating the consequences of constraints. *Nat Rev Microbiol.* 2004; 2(11):886–97. <https://doi.org/10.1038/nrmicro1023> PMID: 15494745
13. Feist AM, Henry CS, Reed JL, Krummenacker M, Joyce AR, Karp PD, et al. A genome-scale metabolic reconstruction for *Escherichia coli* K-12 MG1655 that accounts for 1260 ORFs and thermodynamic

- information. *Mol Syst Biol* [Internet]. 2007 Jan 1 [cited 2018 Jan 30]; 3(1):121. Available from: <http://www.ncbi.nlm.nih.gov/pubmed/17593909>
14. Reed JL, Palsson BØ. Thirteen Years of Building Constraint-Based In Silico Models of *Escherichia coli*. *J Biotechnol*. 2003; 185(9):2692–9.
 15. Weaver DS, Keseler IM, Mackie A, Paulsen IT, Karp PD. A genome-scale metabolic flux model of *Escherichia coli* K–12 derived from the EcoCyc database. *BMC Systems Biol* [Internet]. 2014; 8(79):1–24. Available from: <http://www.biomedcentral.com/1752-0509/8/79>
 16. Rios-Esteva R, Lange BM. Experimental and mathematical approaches to modeling plant metabolic networks. *Phytochemistry*. 2007; 68(16–18):2351–74. <https://doi.org/10.1016/j.phytochem.2007.04.021> PMID: 17561179
 17. Arturo J, Mora M. System biology: Mathematical modeling of biological systems. *Int J Adv Res Comput Eng Technol*. 2016; 5(8):2243–6.
 18. VOLKENSTEIN MV. *Mathematical Modeling of Biological Processes. Physics and Biology*. Springer; 2012. 154 p.
 19. Nikoloski Z, Perez-Storey R, Sweetlove LJ. Inference and prediction of metabolic network fluxes. *Plant Physiol*. 2015; 169:1443–55. <https://doi.org/10.1104/pp.15.01082> PMID: 26392262
 20. Fiévet JB, Dillmann C, Curien G, de Vienne D. Simplified modelling of metabolic pathways for flux prediction and optimization: lessons from an in vitro reconstruction of the upper part of glycolysis. *Biochem J* [Internet]. 2006; 396(2):317–26. Available from: <http://www.ncbi.nlm.nih.gov/pubmed/16460310> <https://doi.org/10.1042/BJ20051520> PMID: 16460310
 21. Antoniewicz MR, Stephanopoulos G, Kelleher JK. Evaluation of regression models in metabolic physiology: Predicting fluxes from isotopic data without knowledge of the pathway. *Metabolomics*. 2006; 2(1):41–52. <https://doi.org/10.1007/s11306-006-0018-2> PMID: 17066125
 22. Almquist J, Cvijovic M, Hatzimanikatis V, Nielsen J. Kinetic models in industrial biotechnology—Improving cell factory performance. *Metab Eng* [Internet]. 2014; 24:38–60. Available from: <https://doi.org/10.1016/j.ymben.2014.03.007> PMID: 24747045
 23. Steuer R, Gross T, Selbig J, Blasius B. Structural kinetic modeling of metabolic networks. *Proc Natl Acad Sci U S A* [Internet]. 2006 Aug 8 [cited 2018 Feb 6]; 103(32):11868–73. Available from: <http://www.ncbi.nlm.nih.gov/pubmed/16880395> <https://doi.org/10.1073/pnas.0600013103> PMID: 16880395
 24. Srinivasan S, Cluett WR, Mahadevan R. Constructing kinetic models of metabolism at genome-scales: A review. *Biotechnol J*. 2015; 10(9):1345–59. <https://doi.org/10.1002/biot.201400522> PMID: 26332243
 25. Covert MW, Famili I, Palsson BO. Identifying Constraints that Govern Cell Behavior: A Key to Converting Conceptual to Computational Models in Biology? *Biotechnol Bioeng*. 2003; 84(7):763–72. <https://doi.org/10.1002/bit.10849> PMID: 14708117
 26. Vijayakumar S, Conway M, Lió P, Angione C. Seeing the wood for the trees: a forest of methods for optimization and omic-network integration in metabolic modelling. *Brief Bioinform*. 2018; 19(6):1218–35. <https://doi.org/10.1093/bib/bbx053> PMID: 28575143
 27. Cornish-Bowden A and Wharton C W. *Enzyme kinetics (In Focus)*. oxford: IRL press ltd; 1988.
 28. Teusink B, Passarge J, Reijenga CA, Esgalhado E, van der Weijden CC, Schepper M, et al. Can yeast glycolysis be understood in terms of in vitro kinetics of the constituent enzymes? Testing biochemistry. *Eur J Biochem* [Internet]. 2000 Sep; 267(17):5313–29. Available from: <http://www.ncbi.nlm.nih.gov/pubmed/10951190> PMID: 10951190
 29. Bisswanger H. Enzyme assays. *Perspect Sci* [Internet]. 2014; 1:41–55. Available from: <http://dx.doi.org/10.1016/j.pisc.2014.02.005>
 30. Wright BE, Butler MH, Albe KR. Systems analysis of the tricarboxylic acid cycle in *dictyostelium discoideum*. I. The basis for model construction. *J Biol Chem*. 1992; 267(5):3101–5. PMID: 1737766
 31. Albe KR, Wright BE. Systems Analysis of the Tricarboxylic Acid Cycle in *Dictyostelium discoideum* II. control Analysis. *J Biol Chem*. 1992; 267(No. 5, Issue of February 15):3106–14. PMID: 1737767
 32. Orth JD, Thiele I, Palsson BO. What is flux balance analysis? *Nat Biotechnol* [Internet]. 2010; 28(3):245–8. Available from: <https://doi.org/10.1038/nbt.1614> PMID: 20212490
 33. Wiechert W. 13C Metabolic Flux Analysis. *Metab Eng* [Internet]. 2001 Jul; 3(3):195–206. Available from: <https://www.sciencedirect.com/science/article/pii/S1096717601901879> <https://doi.org/10.1006/mben.2001.0187> PMID: 11461141
 34. Edwards JS, Palsson BO. The *Escherichia coli* MG1655 in silico metabolic genotype: Its definition, characteristics, and capabilities. *Proc Natl Acad Sci*. 2002; 97(10):5528–33.
 35. Jamshidi N, Palsson B. Investigating the metabolic capabilities of *Mycobacterium tuberculosis* H37Rv using the in silico strain iNJ661 and proposing alternative drug targets. *BMC Syst Biol*. 2007; 1(26):1–20.

36. Claudia S, Quintero JC. Flux Balance Analysis in the Production of Clavulanic Acid by *Streptomyces clavuligerus*. *Biotechnol Prog*. 2015; 31(5):1226–36. <https://doi.org/10.1002/btpr.2132> PMID: [26171767](https://pubmed.ncbi.nlm.nih.gov/26171767/)
37. Christensen B, Nielsen J. Metabolic Network Analysis of *Penicillium chrysogenum* Using C-Labeled Glucose. *Biotechnol Bioeng*. 2000; 68(6):652–9. PMID: [10799990](https://pubmed.ncbi.nlm.nih.gov/10799990/)
38. Chen X, Alonso AP, Allen, Doug K, Reed JL, Shachar-Hill Y. Synergy between ¹³C-metabolic flux analysis and flux balance analysis for understanding metabolic adaption to anaerobiosis in *E. coli*. *Metab Eng* [Internet]. 2010; 13(1):38–48. Available from: <https://doi.org/10.1016/j.ymben.2010.11.004> PMID: [21129495](https://pubmed.ncbi.nlm.nih.gov/21129495/)
39. de Graaf AA, Mahle M, Möllney M, Wiechert W, Stahmann P, Sahm H. Determination of full ¹³C isotope distributions for metabolic flux analysis using heteronuclear spin echo difference NMR spectroscopy. *J Biotechnol*. 2000; 77(1):25–35. PMID: [10674212](https://pubmed.ncbi.nlm.nih.gov/10674212/)
40. Mead CACMHGC, Chopra I. *Organic Acids: Chemistry, Antibacterial Activity and Practical Applications*. *Adv Microb Physiol*. 1991; 32:87–108. PMID: [1882730](https://pubmed.ncbi.nlm.nih.gov/1882730/)
41. Alsaheb RAA, Aladdin A, Othman NZ, Malek RA, Leng OM, Aziz R, et al. Lactic acid applications in pharmaceutical and cosmeceutical industries. *J Chem Pharm Res*. 2015; 7(10):729–35.
42. Weissman KJ, Leadlay PF. Combinatorial biosynthesis of reduced polyketides. *Nat Rev Microbiol*. 2005; 3(12):925–36. <https://doi.org/10.1038/nrmicro1287> PMID: [16322741](https://pubmed.ncbi.nlm.nih.gov/16322741/)
43. Awan AR, Blount BA, Bell DJ, Shaw WM, Ho JCH, McKiernan RM, et al. Biosynthesis of the antibiotic nonribosomal peptide penicillin in baker's yeast. *Nat Commun* [Internet]. 2017; 8(May):1–8. Available from: <http://dx.doi.org/10.1038/ncomms15202>
44. Haris S, Fang C, Bastidas-Oyanedel JR, Prather KJ, Schmidt JE, Thomsen MH. Natural antibacterial agents from arid-region pretreated lignocellulosic biomasses and extracts for the control of lactic acid bacteria in yeast fermentation. *AMB Express* [Internet]. 2018; 8(1):1–7. Available from: <https://doi.org/10.1186/s13568-017-0531-x>
45. Khattak WA, Ul-Islam M, Ullah MW, Yu B, Khan S, Park JK. Yeast cell-free enzyme system for bio-ethanol production at elevated temperatures. *Process Biochem* [Internet]. 2014; 49(3):357–64. Available from: <http://dx.doi.org/10.1016/j.procbio.2013.12.019>
46. Zhang YHP, Sun J, Zhong JJ. Biofuel production by in vitro synthetic enzymatic pathway biotransformation. *Curr Opin Biotechnol* [Internet]. 2010; 21(5):663–9. Available from: <https://doi.org/10.1016/j.copbio.2010.05.005> PMID: [20566280](https://pubmed.ncbi.nlm.nih.gov/20566280/)
47. Zhang YHP. Renewable carbohydrates are a potential high-density hydrogen carrier. *Int J Hydrogen Energy* [Internet]. 2010; 35(19):10334–42. Available from: <http://dx.doi.org/10.1016/j.ijhydene.2010.07.132>
48. Yim H, Haselbeck R, Niu W, Pujol-Baxley C, Burgard A, Boldt J, et al. Metabolic engineering of *Escherichia coli* for direct production of 1,4-butanediol. *Nat Chem Biol* [Internet]. 2011; 7(7):445–52. Available from: <https://doi.org/10.1038/nchembio.580> PMID: [21602812](https://pubmed.ncbi.nlm.nih.gov/21602812/)
49. Anderson LA, Ahsanul Islam M, Prather KLJ. Synthetic biology strategies for improving microbial synthesis of “green” biopolymers. *J Biol Chem* [Internet]. 2018; 293:5053–61. Available from: <https://doi.org/10.1074/jbc.TM117.000368> PMID: [29339554](https://pubmed.ncbi.nlm.nih.gov/29339554/)
50. Lee JW, Na D, Park JM, Lee J, Choi S, Lee SY. systems metabolic engineering of microorganisms for natural and non-natural chemicals. *Nat Chem Biol* [Internet]. 2012; 8(6):536–46. Available from: <https://doi.org/10.1038/nchembio.970> PMID: [22596205](https://pubmed.ncbi.nlm.nih.gov/22596205/)
51. Zeng J, Teo J, Banerjee A, Chapman TW, Kim J, Sarpeshkar R. A Synthetic Microbial Operational Amplifier. *ACS Synth Biol* [Internet]. 2018; 7(9):2007–13. Available from: <https://doi.org/10.1021/acssynbio.8b00138> PMID: [30152993](https://pubmed.ncbi.nlm.nih.gov/30152993/)
52. Liu Jingjing, Li Jianghua Shin Hyun-dong, Liu Long, Guocheng Du JC. Protein and metabolic engineering for the production of organic acids. *Bioresour Technol* [Internet]. 2017 Sep 1 [cited 2017 Oct 6]; 239:412–21. Available from: <http://www.sciencedirect.com/science/article/pii/S0960852417305424?via%3Dihub> <https://doi.org/10.1016/j.biortech.2017.04.052> PMID: [28538198](https://pubmed.ncbi.nlm.nih.gov/28538198/)
53. Hassoun MH. Fundamentals of Artificial Neural Networks. *Proc IEEE*. 1996 Jun; 84(6):906.
54. Jain AK, Mao J, Mohiuddin KM. Artificial neural networks: A tutorial. *Computer* (Long Beach Calif). 1996; 29(3):31–44.
55. Kolanoski H. Application of artificial neural networks in particle physics. *Nucl Instruments Methods Phys Res Sect A*. 1995; 367:14–20.
56. Giuseppe Carleo MT. Solving the quantum many-body problem with artificial neural networks. *Science* (80-). 2017; 355(6325):602–6.

57. LIU ZeLin PENG ChangHui, XIANG WenHua, TIAN DaLun, DENG XiangWen ZM. Application of artificial neural networks in global climate change and ecological research: An overview. *Chinese Sci Bull.* 2010; 55(34):3853–63.
58. Pawul M, Śliwka M. Application of artificial neural networks for prediction of air pollution levels in environmental monitoring. *J Ecol Eng.* 2016; 17(4):190–6.
59. Ahmed Gamal El-Din, Daniel W Smith and MGE-D. The application of artificial neural network in wastewater treatment. *J Environ Eng Sci.* 2004; 3:81–95.
60. Kamruzzaman SM, Jehad Sarkar AM. A new data mining scheme using artificial neural networks. *Sensors.* 2011; 11(5):4622–47. <https://doi.org/10.3390/s110504622> PMID: 22163866
61. Eide Å, Johansson R, Lindblad T, Lindsey CS. Data mining and neural networks for knowledge discovery. *Nucl Instruments Methods Phys Res Sect A Accel Spectrometers, Detect Assoc Equip.* 1997; 389(1–2):251–4.
62. Schmidhuber J. Deep Learning in neural networks: An overview. *Neural Networks [Internet].* 2015; 61:85–117. Available from: <https://doi.org/10.1016/j.neunet.2014.09.003> PMID: 25462637
63. Raman K, Chandra N. Flux balance analysis of biological systems: Applications and challenges. *Brief Bioinform.* 2009; 10(4):435–49. <https://doi.org/10.1093/bib/bbp011> PMID: 19287049
64. Allen DK, Libourel IGL, Shachar-Hill Y. Metabolic flux analysis in plants: Coping with complexity. *Plant, Cell Environ.* 2009; 32(9):1241–57.
65. Vasilakou E, Machado D, Theorell A, Rocha I, Nöh K, Oldiges M, et al. Current state and challenges for dynamic metabolic modeling. *Curr Opin Microbiol.* 2016; 33(1):97–104.
66. Rohwer JM. Kinetic modelling of plant metabolic pathways. *J Exp Bot.* 2012; 63(6):2275–92. <https://doi.org/10.1093/jxb/ers080> PMID: 22419742
67. Rosenblatt F. The perceptron: A probabilistic model for information storage and organization in the brain. *Psychol Rev.* 1958; 65(6):386–408. PMID: 13602029
68. Hornik K, Maxwell S, White H. Multilayer Feedforward Networks are Universal Approximators. *Neural Networks [Internet].* 1989 [cited 2018 Jan 29]; 2:359–66. Available from: https://ac.els-cdn.com/0893608089900208/1-s2.0-0893608089900208-main.pdf?_tid=2e455254-04f2-11e8-acb3-00000aacb35d&acdnat=1517230064_28e5e7c6145756cbc7aa95e108aa024c
69. Venables WN, Ripley B. D. *Modern Applied Statistics with S-Plus [Internet].* 4th ed. Springer. New York: Springer; 2002. Available from: <http://www.stats.ox.ac.uk/pub/MASS4>
70. Günther F, Fritsch S. neuralnet: Training of Neural Networks. *R J.* 2010; 2(1):30–8.
71. Bergmeir C, Benitez JM. Neural Networks in R Using the Stuttgart Neural Network Simulator: RSNNS. *J Stat Softw.* 2012; 46(7):1–26.
72. Gupta R, Rathi P, Gupta N, Bradoo S. Lipase assays for conventional and molecular screening: an overview. *Biotechnol Appl Biochem.* 2003; 37(1):63.
73. Schmeier S, Hakenberg J, Klipp E, Leser U, Kowald A. Finding Kinetic Parameters Using Text Mining. *Omi A J Integr Biol.* 2004; 8(2):131–52.